Protist, Vol. 150, 383–398, December 1999 © Urban & Fischer Verlag
http://www.urbanfischer.de/journals/protist

Protist

ORIGINAL PAPER

Symbiomonas scintillans gen. et sp. nov. and *Picophagus flagellatus* gen. et sp. nov. (Heterokonta): Two New Heterotrophic Flagellates of Picoplanktonic Size

Laure Guillou[a, 1, 2], Marie-Josèphe Chrétiennot-Dinet[b], Sandrine Boulben[a], Seung Yeo Moon-van der Staay[a, 3], and Daniel Vaulot[a]

[a] Station Biologique, CNRS, INSU et Université Pierre et Marie Curie, BP 74, F-29682 Roscoff Cx, France
[b] Laboratoire d'Océanographie biologique, UMR 7621 CNRS/INSU/UPMC, Laboratoire Arago, O.O.B., B.P. 44, F-66651 Banyuls sur mer Cx, France

Submitted July 27, 1999; Accepted November 10, 1999
Monitoring Editor: Michael Melkonian

Two new oceanic free-living heterotrophic Heterokonta species with picoplanktonic size (< 2 µm) are described. *Symbiomonas scintillans* Guillou et Chrétiennot-Dinet *gen. et sp. nov.* was isolated from samples collected both in the equatorial Pacific Ocean and the Mediterranean Sea. This new species possesses ultrastructural features of the bicosoecids, such as the absence of a helix in the flagellar transitional region (found in *Cafeteria roenbergensis* and in a few bicosoecids), and a flagellar root system very similar to that of *C. roenbergensis, Acronema sippewissettensis,* and *Bicosoeca maris*. This new species is characterized by a single flagellum with mastigonemes, the presence of endosymbiotic bacteria located close to the nucleus, the absence of a lorica and a R3 root composed of a 6+3+x microtubular structure. Phylogenetical analyses of nuclear-encoded SSU rDNA gene sequences indicate that this species is close to the bicosoecids *C. roenbergensis* and *Siluania monomastiga*. *Picophagus flagellatus* Guillou et Chrétiennot-Dinet *gen. et sp. nov.* was collected in the equatorial Pacific Ocean. Cells are naked and possess two flagella. This species is characterized by the lack of a transitional helix and lateral filaments on the flagellar tubular hairs, the absence of siliceous scales, two unequal flagella, R1 + R3 roots, and the absence of a rhizoplast. SSU rDNA analyses place this strain at the base of the Chrysophyceae/Synurophyceae lineages.

Introduction

Within the eukaryotic kingdom, unicellular organisms are probably the most diversified but also the least known, especially when the smaller size classes are considered. Despite the pioneering work of Butcher (1952), who identified algae smaller than 10 µm in size, the ecological importance of very small eukaryotes was recognized in both coastal and oceanic waters less than 20 years ago (Johnson and Sieburth 1982). It is now well established that in oceanic environments, the majority of cells are picoplanktonic, i.e. smaller than 2–3 µm (Li et al. 1983;

[1] Corresponding author;
fax 33-2 98 22 47 57
e-mail Laure.Guillou@ifremer.fr

[2] Present address: Ifremer – Centre de Brest – DRV VP CMM, BP70, F-29280 Plouzané, France
[3] Present address: Universität zu Köln, Botanisches Institut, Lehrstuhl I, Gyrhofstr. 15, D-50931 Köln, Germany

1434-4610/99/150/04-383 $ 12.00/0

Platt et al. 1983). During the last ten years, investigations of oceanic picoeukaryote diversity have led to descriptions of new species, genera, or even classes, such as the Pelagophyceae Andersen et Saunders (Andersen et al. 1993) and the Bolidophyceae Guillou et Chrétiennot-Dinet (Guillou et al. 1999). Picoeukaryote communities are undoubtedly an important reservoir of unknown species and unknown lineages. Most of oceanic picoeukaryotes described to date are photosynthetic. Nevertheless, some recent studies have reported that heterotrophic picoflagellates could be important grazers in oceans (Caron et al. 1999; Reckermann and Veldhuis 1997).

We describe in the present study two new oceanic flagellates with picoplanktonic size, *Symbiomonas scintillans* gen. et sp. nov and *Picophagus flagellatus* gen. et sp. nov., both are heterotrophic and phagotrophic. They are very small, with an average size diameter of 1.4 and 1.8 µm respectively. Their ultrastructure and 18S rDNA gene sequence are presented in this study.

Results

Morphology and Ultrastructure of *S. scintillans* (strains RCC24 and RCC25)

Strains RCC24 and RCC25, isolated respectively in the equatorial Pacific and in the Mediterranean Sea, have a similar morphology and ultrastructure. Most of the cells swim in a straight line with the flagellum extended forward. Cells that are stopped or swim at a reduced speed flicker. In old cultures, most cells do not swim. Cells are spherical or ovoid (Fig. 1A, B). They measure 1.1–1.5 (mean = 1.3) µm in width and 1.2–1.5 (mean = 1.4) µm in length. They are naked, without cytostome or protruding lips. They possess a single flagellum, bearing two rows of tripartite mastigonemes, composed of a flexible basal section, followed by a tubular part and terminated by two relatively long hairs (Fig. 1C). No lateral filaments are observed on these mastigonemes. Two mitochondria with tubular cristae are located symmetrically against the basal body (Fig. 1D). The flagellar apparatus is composed of one basal body that bears the emerging flagellum and of microtubular roots. Fibrous roots are absent. The flagellar transitional region contains a single basal plate with a prominent central axosome and a transitional helix is absent (Fig. 1E). The R3 microtubular root is well developed and anchored to the basal body by a striated band (Fig. 2D). It is composed of three microtubules – referred to as “a”, “b”, “c” by homology with those of *Bicosoeca maris* (Moestrup and Thomsen 1976) and *Cafeteria roenbergensis* (O’Kelly and Patterson 1996) – plus a row of 6 microtubules (Fig. 2C, D) and an additional microtubule, labelled “x” (Fig. 2C, D). The R3 root forms an arc in the dorsal part of the cell (Fig. 1B and Fig. 2E). The R1 root is also present and composed of at least two microtubules (Fig. 2A, D). A few sections show effective phagotrophy of heterotrophic bacteria (Fig. 1D, Fig. 2A). Moreover, several (generally more than two) bacteria are enclosed inside the endoplasmic reticulum which is continuous with the outer membrane of the nucleus (Fig. 1D). These kind of bacteria have never been observed outside the cell and we did not find any sign of attack by digestive enzymes. Strains RCC24 and RCC25 have the same ultrastructural characteristics, except that more endobacteria (sometimes in excess of six) are found in strain RCC25. Cysts or resistant cells have not been observed.

Morphology and Ultrastructure of *P. flagellatus* (strain RCC22)

All cells swim energetically, with a large sinusoidal motion. The long flagellum is easily visible with optical microscopy, and placed in front of the cell. The vegetative cells are spherical or ovoid (Fig. 3A). Their size is quite variable, 1.1–2.5 (mean = 1.8) µm in width and 1.4–2.5 (mean = 2) µm in length. The cells are naked and possess two flagella, the longer one bearing two rows of tripartite mastigonemes. Two filaments appear at the end of each mastigoneme, but lateral filaments are absent (Fig. 3C). Different types of flagellar ends have been observed in our preparations: with a terminal swelling (Fig. 3A) and with or without an acronema (not shown). One nucleus, one Golgi body and two mitochondria are present (Fig. 3D, E). The two mitochondria contain tubular cristae and are placed symmetrically against the nucleus (Fig. 3E). Neither a transitional helix (Fig. 3B), nor a fibrous root have been observed. The two basal bodies (bb1 and bb2 for the short and long flagella, respectively), are placed at right angles of each other (Fig. 4A). bb1 is close to bb2, and bb2 close to one mitochondrion (Fig. 4A) and the nucleus (Fig. 4A). Both basal bodies are anchored by a dense matrix (Fig. 3D, and Fig. 4A). A R1 root is present, whose origin is in close proximity to bb2 (Fig. 4A, B). It is composed of a row of at least 6 microtubules (Fig. 4C, D, E). The R3 root originates next to bb1 and bb2, and is parallel to bb2 (Fig. 5A). It is composed of a semi-circle of at least 8 microtubules (Fig. 4A and Fig. 5B, C, D, E). Two of them seem to be shorter than the others (Fig. 5C, D). R2 or R4 roots were not observed.

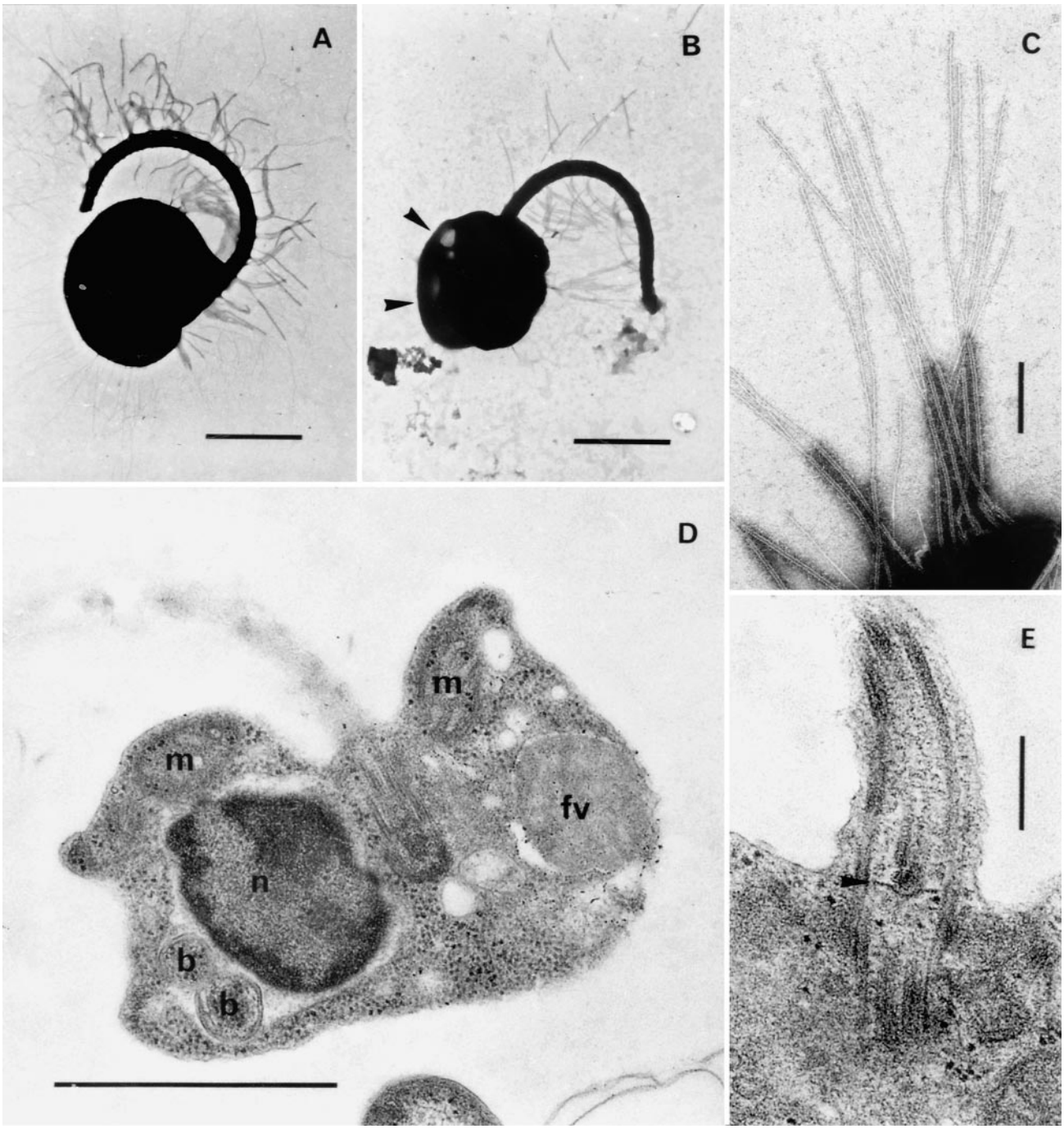

Figure 1. *Symbiomonas scintillans.* General morphology and ultrastructure. **A** – A unique flagellum bearing mastigonemes emerges from the posterior part of the cell. Scale bar: 1 µm. **B** – The R3 flagellar root is visible on entire cells, located in the dorsal part of the cell (small arrowheads). Scale bar: 1µm. **C** – Detail of the mastigonemes, which are tripartite, i.e. with a basal flexible part, followed by a tubular section and terminated by two relatively long hairs. Note the absence of lateral filaments. Scale bar: 200 nm. **D** – General organization of the cells, with two mitochondria (m), a nucleus (n) and two endosymbiotic bacteria (b). The bacteria are enclosed within an endoplasmic reticulum, which is continuous with the outer membrane of the nuclear envelope. A food vacuole (fv) is also present. Scale bar: 1 µm. **E** – Longitudinal section through the transitional region of the flagellum. Note the presence of the transitional plate (small arrow) with a prominent central axosome, and the absence of a transitional helix. Scale bar: 200 nm.

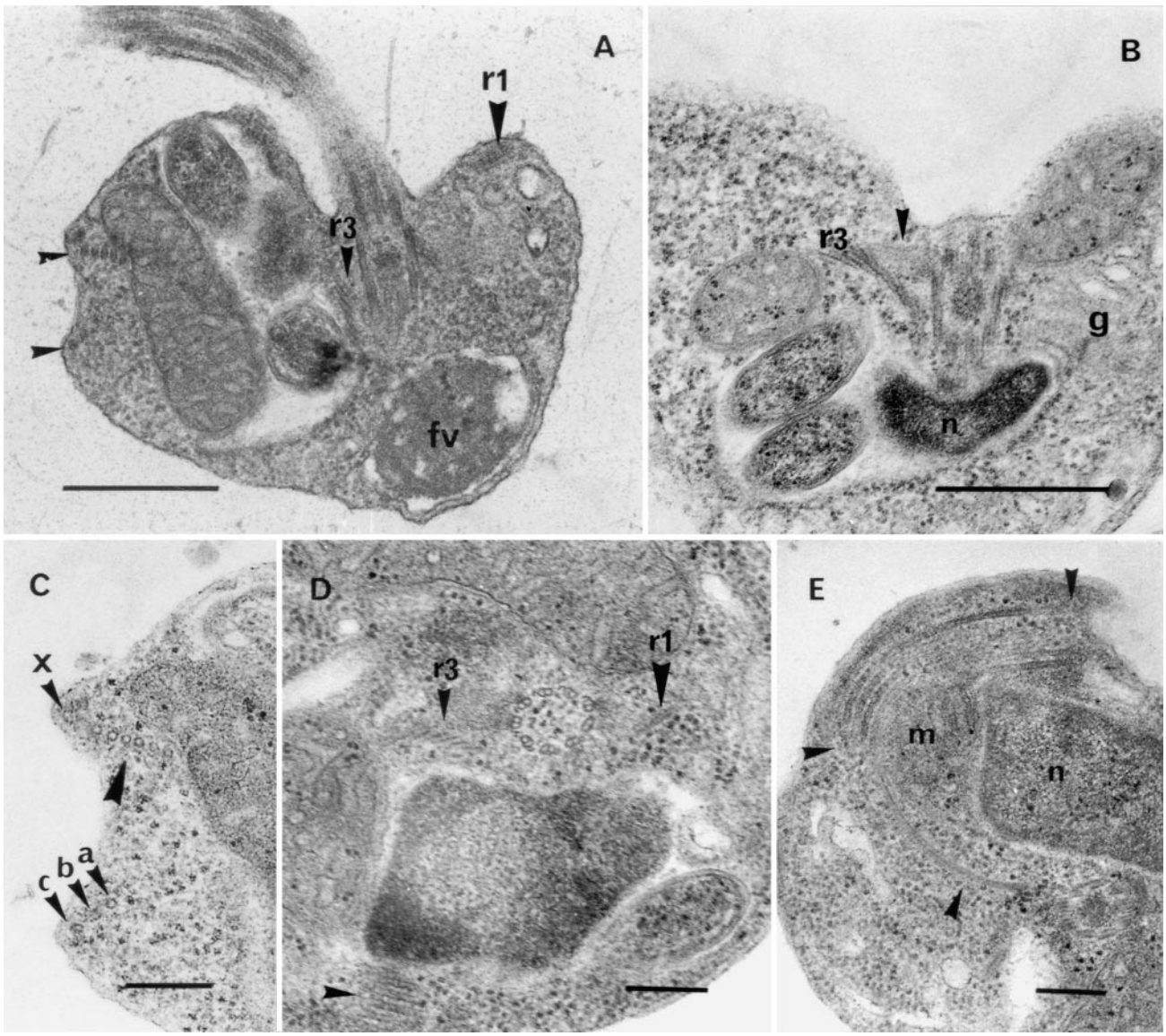

Figure 2. *Symbiomonas scintillans.* Details of the flagellar roots. **A** – Longitudinal section showing the departure of the R1 (large arrowhead) and R3 roots (3 small arrowheads) near the basal body. Scale bar: 500 nm. **B** – Oblique section in the flagellar insertion region, showing the departure of the R3 root microtubules from the vicinity of the basal body. The nucleus (n) makes a depression around the basal body. The Golgi apparatus (g) is also visible adjacent to the nucleus (n). A striated band (small arrow) anchors the R3 root to the basal body. The relative position of the endobacteria with respect to the nucleus is clearly visible on this micrograph. Scale bar: 500 nm. **C** – Longitudinal section through the dorsal part of the cell. The R3 root, composed of a row of 6 microtubules (large arrow) and the "a", "b", "c" microtubules, is visible between the plasmalemma and the mitochondrion. An "x" microtubule is also present. Scale bar: 200 nm. **D** – Longitudinal section through the cell. The R3 root departure is visible in the vicinity of the basal body and reappears on the dorsal side of the cell (small arrows). The R1 root (large arrow) is located in the ventral part of the cell. Scale bar: 200 nm. **E** – Longitudinal section inside the cell. The row of 6 microtubules which compose the R3 root and the "x" microtubules begins at the central part of the cell, then makes an arc in the dorsal part of the cell around both the nucleus (n) and mitochondrion (m).

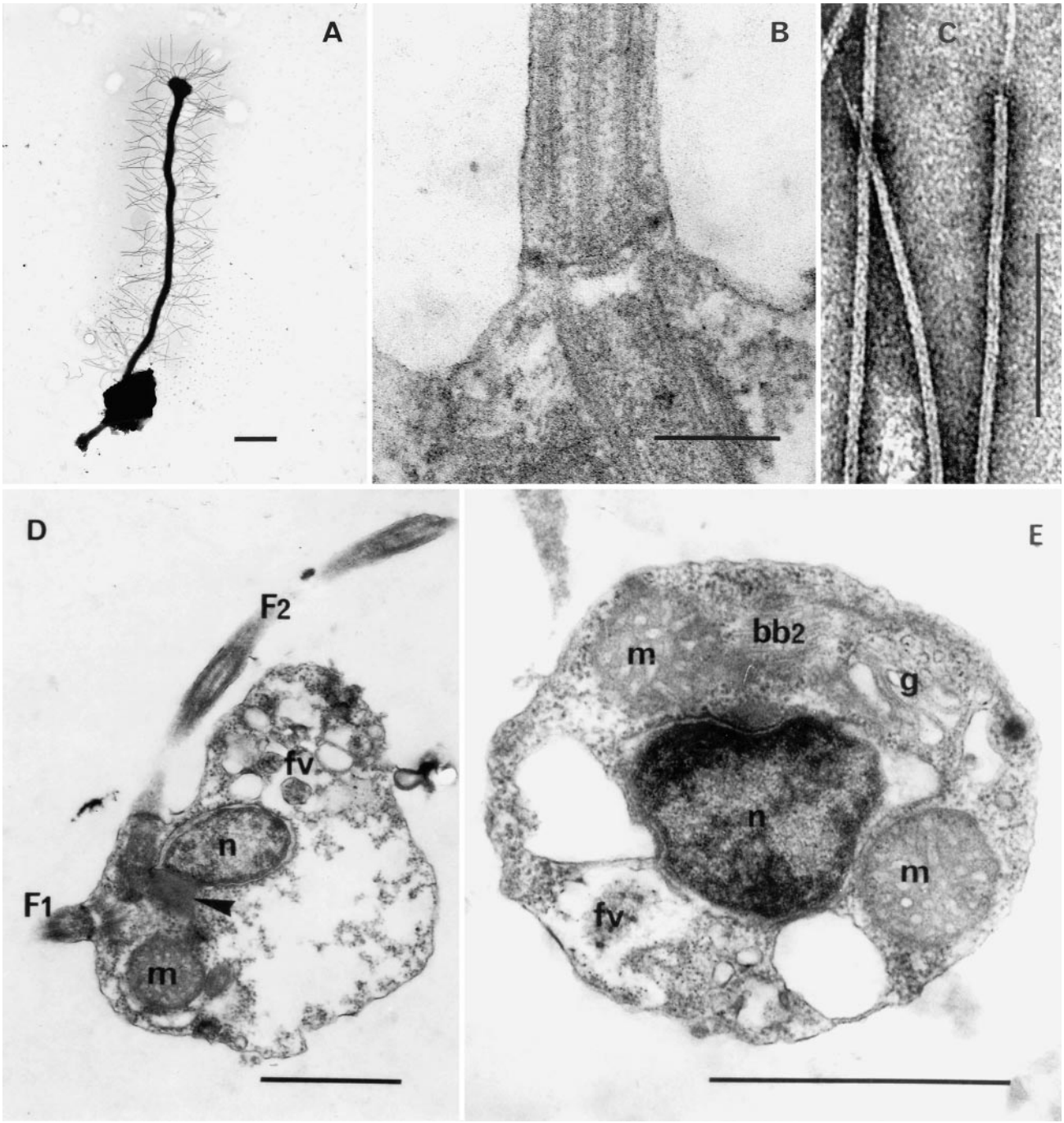

Figure 3. *Picophagus flagellatus*. General morphology and ultrastructure. **A** – General morphology, showing two emerging flagella, the longer one bearing mastigonemes. The average size of the cell is 1.8 µm. Scale bar: 1 µm. **B** – Longitudinal section through the transitional region of the long flagellum. Note the absence of a transitional helix. Scale bar: 200 nm. **C** – Detail of the mastigonemes. Note the absence of lateral filaments and the presence of terminal filaments. Scale Bar: 200 nm. **D** – Longitudinal section through the long (F2) and the short (F1) flagella. The basal body of the long flagellum is anchored to the nucleus (n) by a dense matrix (arrow). A food vacuole (fv) and a mitochondrion (m) are also present. Scale bar: 1 µm. **E** – Section through the cell, showing the basal body of the short flagellum (bb2), the two mitochondria (m), the nucleus (n) and the Golgi apparatus (g). The two mitochondria are positioned symmetrically on each side of the nucleus. Note also the presence of a digestive food vacuole (fv). Scale bar: 1 µm.

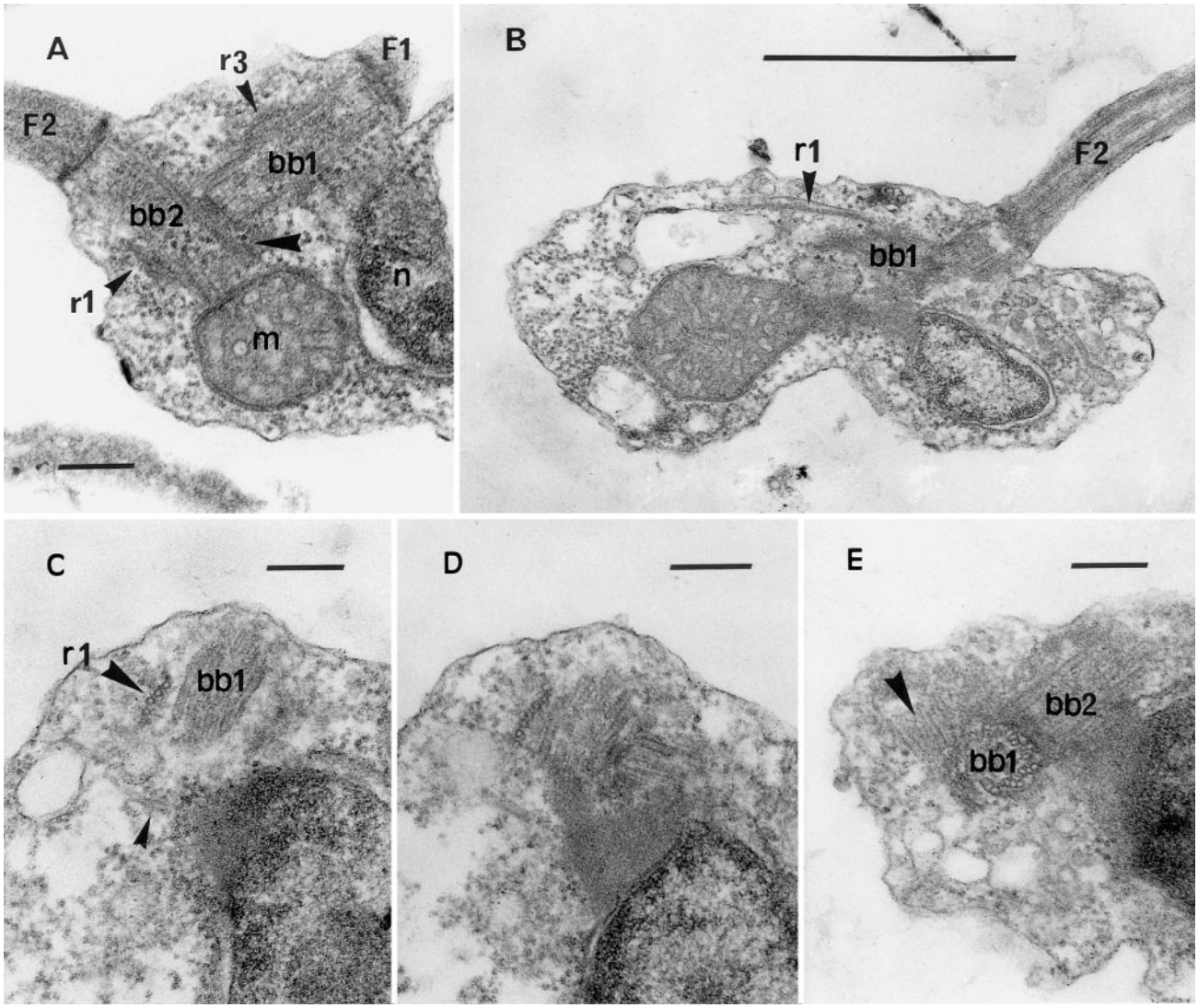

Figure 4. *Picophagus flagellatus*. Flagellar apparatus, with special reference to the R1 microtubular roots. **A** – Relative position of the two basal bodies, which make an angle of 90°. Note the presence of the basal body of the long flagellum (bb1) next to the nucleus, and the basal body of the short flagellum (bb2) which ends next to a mitochondrion. The two basal bodies are linked by connecting fibers (large arrow). The beginning of R1 and R3 roots are visible (small arrows). Note also the absence of a transitional helix. Scale bar: 200 nm. **B** – Oblique section through the long flagellum and the two basal bodies. Microtubules (arrow), belonging to the R1 root, originate next to bb1. Scale bar: 1 µm. **C, D** – Serial micrographs through bb1, showing the R1 root in transversal sections (large arrows). The R1 root is composed of a row of at least 6 microtubules. An additional microtubule (small arrows) is also visible. Scale bar: 200 nm. **E** – Transverse section through the bb1, showing the beginning of the R1 root (large arrow) and the relative position of bb2. Scale bar: 200 nm.

Molecular Analysis

Sequences of the SSU rDNA of *S. scintillans* and *P. flagellatus* group with those of the Heterokonta (named also stramenopiles, Patterson 1989) by both distance analyses (maximum likelihood, ML, and neighbor-joining, NJ) and parsimony methods (Fig. 6). The tree topology and the branching order between all heterokonts is conserved in all phylogenetic analyses, with the exception of the Eustigmatophyceae (which are placed as a sister group of the Raphidophyceae/Phaeophyceae lineages in parsimony analysis), and of the position of the *Paraphysomonas* spp. inside the chrysophycean lineage

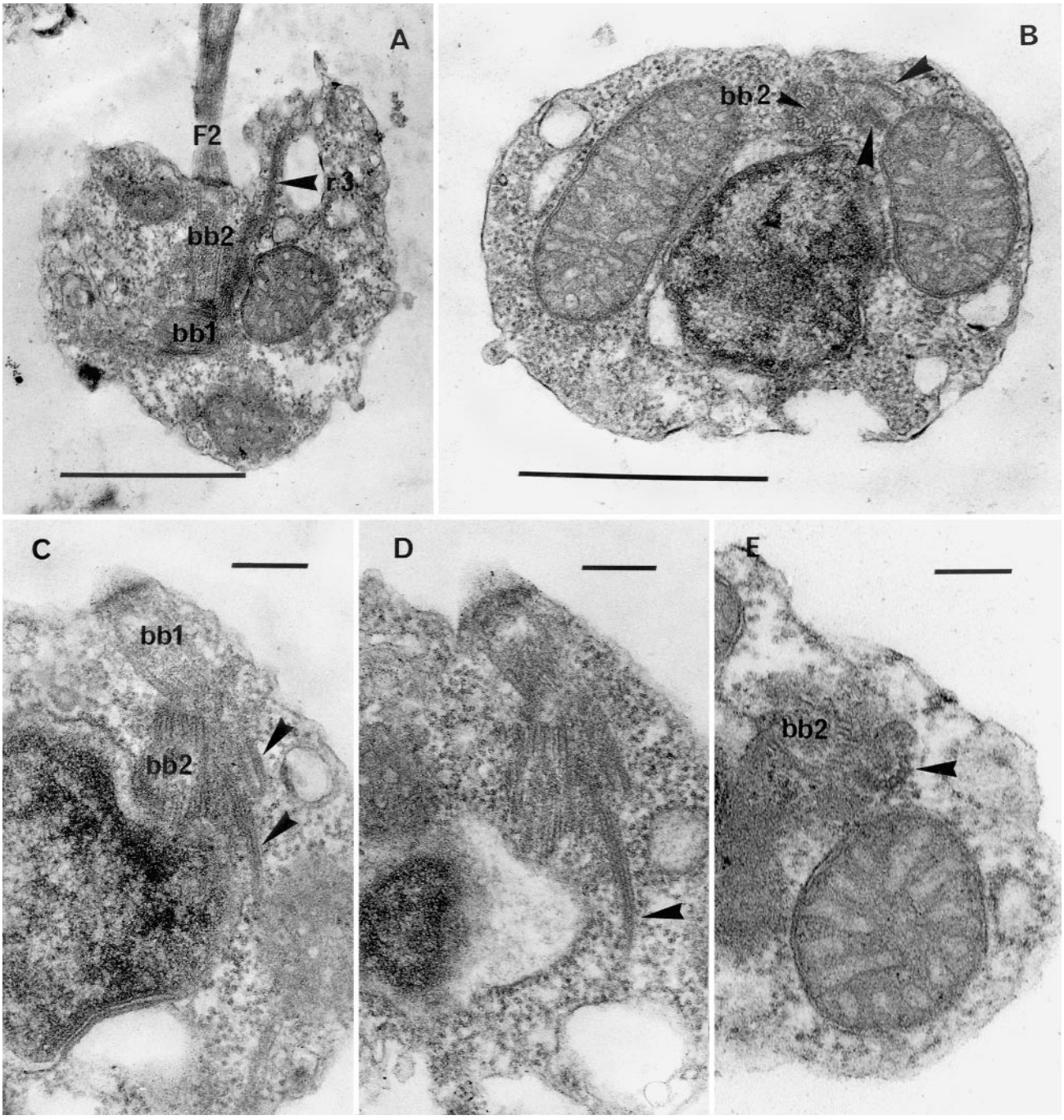

Figure 5. *Picophagus flagellatus*. Flagellar apparatus, with special reference to the R3 microtubular roots. **A** – Longitudinal section through the long flagellum (F2). The R3 root (large arrow) originates next to bb1 and bb2. Scale bar: 1 µm. **B** – Transverse section through the cell and bb2, showing the R3 root departure (large arrows). Scale bar: 1 µm. **C, D** – Serial micrographs through bb1 (in longitudinal sections) and bb2 (in oblique sections) showing the R3 root departure (large arrow). Scale bar: 200 nm. **E** – bb2 and the R3 root (large arrow) in cross-section. The R3 root is composed of a row of 8 microtubules which form a semicircle. Scale bar: 200 nm.

(which are placed as the first lineage to emerge after *P. flagellatus* in NJ analysis). *P. flagellatus* is placed at the origin of the Chrysophyceae/Synurophyceae with the database used. This affiliation is supported by all phylogenetic analyses used and bootstrap values of more than 70% in parsimony and NJ methods. When more chrysophycean sequences are analyzed, (alignment provided by RA Andersen; Andersen et al. 1999), the *P. flagellatus* sequence is always placed at the base of the chrysophycean lineages.

Strains RCC24 and RCC25 are closely related, with only 7 different nucleotides in their SSU rDNA sequences. The tree topology obtained by the ML method (Fig. 7) is similar to that obtained in NJ and parsimony analyses. The opalinids are placed near the basal group. One clade, well supported by bootstrap analyses (respectively 76% in NJ and 96% in parsimony), is composed of 1) the bicosoecids + *Proteromonas* + *Blastocystis* spp. closely related and both included in the clade within the oomycetes, the hyphochytrids and *Developayella*, and 2) the thraustochytrids and the labyrinthulids clade. All phylogenetic methods support that the *S. scintillans* sequences clustered within the bicosoecid clade (Fig. 7).

Discussion

Both species belong to the Heterokonta based upon phylogenetical analyses and ultrastructural characteristics, such as the presence of tripartite tubular hairs on the immature flagellum (for the terminology of the flagellar apparatus elements, see Andersen et al. 1991) or the presence of mitochondria with tubular cristae. The two trees presented (Fig. 6, 7) are coherent with others previously published (Andersen et al. 1998; Dick et al. 1999; Guillou et al. 1999; Honda et al. 1999; Saunders et al. 1997). The heterokont tree (Fig. 6) contains a basal heterotrophic part from which all autotrophic heterokont lineages emerge (Leipe et al. 1996). All phylogenetical analyses clearly placed *S. scintillans* inside the bicosoecids, in the basal part of the heterokonts, and *P. flagellatus* at the basal part of the chrysophycean lineage.

Symbiomonas scintillans gen et sp. nov. (Bicosoecid)

The basal heterotrophic group of the Heterokonta is very heterogeneous, although well defined by morphology and trophic characteristics. For example, the genera *Blastocystis* and *Proteromonas* are mostly vertebrate intestine or rectum endosymbionts; some of them are even human parasites (Silberman et al. 1996). However, their general morphology has clearly diverged from the typical biflagellated heterokont unicell. Labyrinthulids, hyphochytrids and oomycetes possess a cell wall during growth and acquire nutrients by absorption (Porter 1990). Some of them are parasitic for example (as within the Oomycota). Inside these lineages, the sole flagellated stage to be observed occurs during zoospore formation (Dick 1990). Until now, free-living flagellates belonging to this basal group are restricted to the newly described *D. elegans* (Tong 1995) and to the bicosoecids. *S. scintillans*, which lacks a transitional helix, can be separated from the Oomycota and *D. elegans*, but also from the opalinids, which are characterized by the presence of a double stranded transitional helix (Barr and Allan 1985; Barr and Désaulniers 1989; Patterson 1985). The absence of a transitional helix has been reported in some bicosoecids, e.g. *C. roenbergensis* and a few *Bicosoeca* (Fenchel and Patterson 1988), but also in some photosynthetic lineages such as the Bolidophyceae or the Raphidophyceae. The most revealing feature of *S. scintillans* is the R3 root structure which is very similar to that of bicosoecids, e.g. *C. roenbergensis* (O'Kelly and Patterson 1996), *B. maris* (Moestrup and Thomsen 1976), and *A. sippewissettensis* (Teal et al. 1998). For both

Figure 6. Distance tree (maximum likelihood method) derived from an alignment of SSU rDNA sequences from different heterokonts. Bootstrap values at the internal branches (100 replicates, values >70% displayed) corresponding to a neighbor-joining and a parsimony analysis respectively. Bold numbers correspond to identical bootstrap values in both analyses. Scale Bar: 0.1% divergence. *P. flagellatus* (RCC22 strain: AF185051) and *S. scintillans* (RCC24 strain: AF185052, RCC25 strain: AF185053) sequences have been aligned with the sequences used in Guillou et al. (1999) completed with the following sequences: *A. belauense* (L13719), *A. tamarense* (X54946), *B. hominis* (U51151), *Blastocystis* sp. (U51152), *C. virguloides* (AF141969), *Chrysosaccus* sp. (AF123300), Guinea pig faeces isolate (U26177), *L. haliotis* (U21338), *N. granulata* (U38903), *N. oculata* (U38902), *O. ranarum* (AF141970), *Ochromonas* sp. (CCMP1278 strain: U42382), *Ochromonas* sp. (CCMP584 strain: U42381), *P. bandaiensis* (AF109322), *P. butcheri* (AF109326), *P. imperforata* (AF109324), *P. lacertae* (U37108), *P. minimum* (Y16238), *S. monomastiga* (AF072883), *T. kinnei* (L34668), and *U. profunda* (L34054).

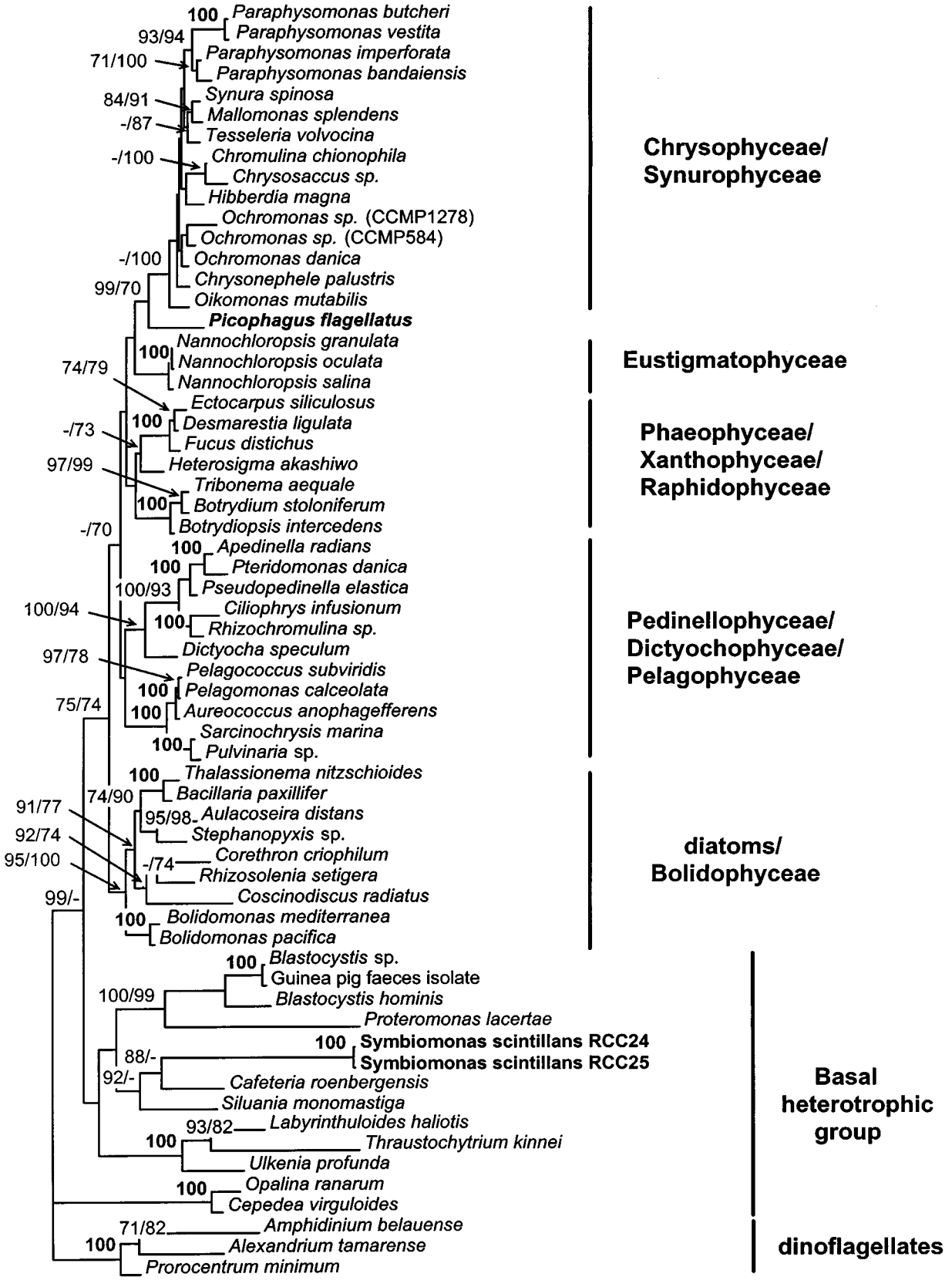
100 Paraphysomonas butcheri
93/94 Paraphysomonas vestita
71/100 Paraphysomonas imperforata
Paraphysomonas bandaiensis
84/91 Synura spinosa
-/87 Mallomonas splendens
Tesseleria volvocina
-/100 Chromulina chionophila
Chrysosaccus sp.
Hibberdia magna
Ochromonas sp. (CCMP1278)
Ochromonas sp. (CCMP584)
-/100 Ochromonas danica
Chrysonephele palustris
99/70 Oikomonas mutabilis
Picophagus flagellatus
Nannochloropsis granulata
100 Nannochloropsis oculata
74/79 Nannochloropsis salina
Ectocarpus siliculosus
100 Desmarestia ligulata
-/73 Fucus distichus
97/99 Heterosigma akashiwo
Tribonema aequale
100 Botrydium stoloniferum
Botrydiopsis intercedens
-/70 100 Apedinella radians
100 Pteridomonas danica
100/93 Pseudopedinella elastica
100/94 Ciliophrys infusionum
100 Rhizochromulina sp.
97/78 Dictyocha speculum
Pelagococcus subviridis
100 Pelagomonas calceolata
75/74 100 Aureococcus anophagefferens
Sarcinochrysis marina
100 Pulvinaria sp.
100 Thalassionema nitzschioides
74/90 Bacillaria paxillifer
91/77 95/98 Aulacoseira distans
92/74 Stephanopyxis sp.
95/100 -/74 Corethron criophilum
Rhizosolenia setigera
99/- Coscinodiscus radiatus
100 Bolidomonas mediterranea
Bolidomonas pacifica
100 Blastocystis sp.
Guinea pig faeces isolate
100/99 Blastocystis hominis
Proteromonas lacertae
100 Symbiomonas scintillans RCC24
Symbiomonas scintillans RCC25
88/- 92/- Cafeteria roenbergensis
Siluania monomastiga
93/82 Labyrinthuloides haliotis
100 Thraustochytrium kinnei
Ulkenia profunda
100 Opalina ranarum
Cepedea virguloides
71/82 Amphidinium belauense
100 Alexandrium tamarense
Prorocentrum minimum
0.1
Chrysophyceae/
Synurophyceae
Eustigmatophyceae
Phaeophyceae/
Xanthophyceae/
Raphidophyceae
Pedinellophyceae/
Dictyochophyceae/
Pelagophyceae
diatoms/
Bolidophyceae
Basal
heterotrophic
group
dinoflagellates

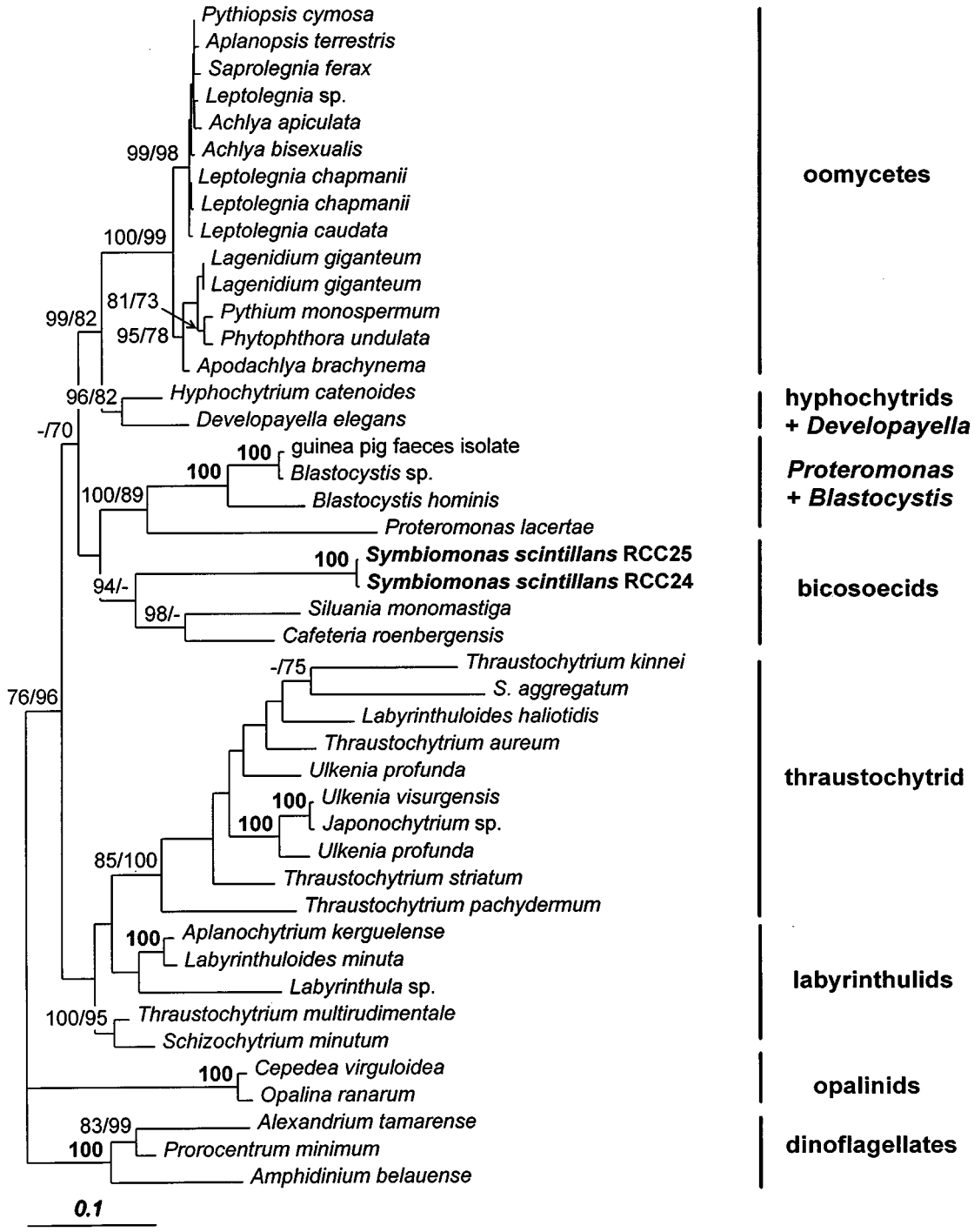

Figure 7. Distance tree (maximum likelihood method) derived from an alignment of SSU rDNA sequences from different species belonging to the basal heterotrophic heterokont lineages. Bootstrap values at the internal branches (100 replicates, values >70% displayed) corresponding to a neighbor-joining and a parsimony analysis respectively. Bold numbers correspond to identical bootstrap values in both analyses. Scale Bar: 0.1% divergence. *S. scintillans* (RCC24 strain: AF185052 and RCC25 strain: AF185053) sequences have been aligned with sequences of *A. apiculata* (AJ238656), *A. bisexualis* (M32705), *A. brachynema* (AJ238663), *A. kerguelense* (AB022103), *A. terrestris* (AJ238658), *B. hominis* (U51152), *Blastocystis* sp. (U51152), *C. roenbergensis* (L27633), *C. virguloidea* (AF141969), *D. elegans* (U37107), *H. catenoides* (X80344), *Japonochytrium* sp. (AB022104), *L. caudata* (AJ238659), *L. chapmanii* (AJ238661, AJ238660), *L. giganteum* (X54266, M54939), *L. haliotis* (U21338), *L. minuta* (L27634),

species, this R3 root is composed of a row of 6 microtubules, 3 microtubules named “a”, “b”, “c” and an additional microtubule named “x”. Consequently, both molecular phylogenetical and ultrastructural characteristics converge to place *S. scintillans* within the bicosoecids.

Nevertheless, *S. scintillans* has several peculiarities when compared to all bicosoecids genera previously described (5 genera in total: *Acronema* Teal et al., *Bicosoeca* James-Clark, *Cafeteria* Fenchel and Patterson, *Pseudobodo* Griessmann, and *Siluania* Karpov et al.). The genus *Bicosoeca* is characterized by the presence of a lorica. The genera *Bicosoeca*, *Acronema*, *Cafeteria* and *Pseudobodo* are characterized by the presence of two flagella, one long one, which bears mastigonemes and a short one, with an adhesive tip. *S. scintillans*, like *Siluania monomastiga* (Karpov et al. 1998), does not have this short adhesive flagellum. *S. scintillans* differs also in the R3 flagellar root, which is composed of 6+3+x microtubules, whereas the combination found in *A. sippewissettensis* (Teal et al. 1998), *C. roenbergensis* (O'Kelly and Patterson 1996) and *B. maris* (Moestrup and Thomsen 1976) is 8+3+x. *S. monomastiga* can be distinguished ultrastructurally from *S. scintillans* by the following features: a second vestigial basal body, a cytostome, protruding lips, a transitional helix, and a very unusual R3 root structure composed of 3+1 microtubules (Karpov et al. 1998). The SSU rDNA gene sequences of *S. scintillans* are very different from those of other bicosoecids, and both share only 82% similarity with those of *C. roenbergensis* and *S. monomastiga* (*C. roenbergensis* and *S. monomastiga* share 88% similarity).

For all these reasons, we have created a new genus and a new species, *S. scintillans*, placed inside the bicosoecids. The SSU rDNA sequences of the two strains from the equatorial Pacific and the Mediterranean Sea differ by only 7 different nucleotides. Therefore, we have grouped them under the same genus and same species. The difference in the number of endobacteria found in both strains could have resulted from a difference in the culture stage at harvest for TEM or could be genotypic.

P. flagellatus gen. et sp. nov. (Chrysophyceae)

The Chrysophyceae contains only two lineages characterized by free-living biflagellates, i.e. the Paraphysomonadaceae (Preisig and Hibberd 1983) and the Ochromonadales (Bourrelly 1968). Both groups contain heterotrophic and autotrophic taxa. The Paraphysomonadaceae are characterized by the presence of silica scales on the cells, which are completely absent in our isolate. The description of Ochromonadales fits best with the general morphology of *P. flagellatus*. The Ochromonadales is well defined by two flagella and the formation of a R3 root, which forms a loop under the short flagellum (or F1) during phagotrophy (Andersen et al. 1999). This row of microtubules may form a feeding basket by interaction with the R4 root, and has been well studied in *Epipyxis pulchra* (Andersen and Wetherbee 1992). Our observations suggest that *P. flagellatus* possesses only 2 microtubular roots, that we have named R1 and R3 by homology. These flagellar roots have opposite orientations inside the cell, the R3 root is observed close to the nucleus, whereas the R1 root is located on the opposite side of the cell. Both seem to have a very reduced length as compared to that of other Ochromonadales, and no evidence has as yet been found for the typical R3 loop under the short flagellum, associated with a R4 root. Consequently, based upon ultrastructural and molecular phylogenetical characteristics, it is impossible to place *P. flagellatus* inside the Ochromonadales or inside the Paraphysomonadaceae. The difficulty to classify this taxon is increased by the lack of a plastid and of the associated pigments, which can provide very useful taxonomical characters. Furthermore, *P. flagellatus* has several unusual specific characteristics for both Chrysophyceae and Synurophyceae lineages such as the absence of a flagellar transitional helix (which is generally well-developed in both the Chrysophyceae and Synurophyceae) and of lateral filaments on the mastigonemes. Because it is difficult to place a taxon solely on the basis of absent characters, we tentatively include *P. flagellatus* within the Chrysophyceae *sensu*

Labyrinthula sp. (AB022105), *Leptolegnia* sp. (AJ238662), *O. ranarum* (AF141970), *P. cymosa* (AJ238657), *P. lacertae* (U37108), *P. monospermum* (AJ238653), *P. undulata* (AJ238654), *S. aggregatum* (AB022106), *S. ferax* (AJ238655), *S. minutum* (AB022108), *S. monomastiga* (AF07883), *T. aureum* (AB022110), *T. kinnei* (L34668), *T. multirudimentale* (AB022111), *T. pachydermum* (AB022113), *T. striatum* (AB022112), *U. profunda* (L34054, AB022114), *U. visurgensis* (AB022116), and unidentified guinea pig faeces isolate (U26177).

stricto. This new genus is characterized by 1) naked free-living unicells, 2) the absence of a helix in the transitional region of the flagella, and 3) the absence of lateral filaments on the mastigonemes.

Phagotrophy and Endosymbiosis

Heterokont algal lineages are assumed to have arisen from a secondary endosymbiosis between a heterotrophic eukaryote and a primitive red alga (Bhattacharya and Medlin 1995; Daugbjerg and Andersen 1997; Delwiche et al. 1995). Based upon the phylogenetic analyses of the nuclear SSU rDNA (originating from the ancestral host), this secondary endosymbiosis is thought to have arisen after the emergence of several strictly heterotrophic lineages (Leipe et al. 1996). If this hypothesis holds true, *S. scintillans* would belong to the basal heterotrophic lineages whereas *P. flagellatus* would have lost its plastid. Both species have presumably kept their ancestral phagotrophic capacity, which is believed to be the crucial element for endosymbiosis events (Raven 1998). Symbiotic endobacteria, such as those probably present in *S. scintillans*, have been reported in several heterokont taxa such as the genus *Paraphysomonas* (Preisig and Hibberd 1983), *Chrysamoeaba radians* (Hibberd 1971), or in *Ochromonas monicis* (Doddema and van der Veer 1983). The intracellular location of all these endobacteria is similar to that of plastids in heterokont autotrophic lineages: they are included inside an endoplasmic reticulum vesicle, which is continuous with the outer membrane of the nuclear envelope.

Potential Ecological Role

Ultrastructural analyses suggest that *P. flagellatus* and *S. scintillans* are potentially phagotrophic. *P. flagellatus* indeed feeds very actively on abundant oceanic primary producers, such as *Synechococcus* and *Prochlorococcus* (Guillou unpublished). Heterotrophic picoflagellates are considered a key element in the oceanic ecosystem, in particular with respect to their role in controlling both bacteria and picophytoplankton. In the case of *S. scintillans*, the capacity to bear endosymbiotic bacteria could provide ecological advantages in oligotrophic waters, especially if the bacteria possess functions that can provide essential nutrients to the host (N_2 fixation for example). Very few free-living heterotrophic picoflagellates have been described (Karpov et al. 1998). Furthermore, some of them have been described from direct observations based only on natural samples, such as the bicosoecids *Pseudobodo minimus* Ruinen (Ruinen 1938). For such small organisms, molecular biology can be very useful, not only for the taxonomist but also for the ecologist who cannot distinguish such taxa with only the optical microscope. Molecular techniques, such as fluorescent *in situ* hybridization (Lim et al. 1999), or PCR detection using rDNA-targeted probes (Penna and Magnani 1999), provide very sensitive tools to detect these tiny species.

Diagnoses

P. flagellatus which belongs to a photosynthetic lineage, is described following the International Botanical code (i.e. with a Latin description) and *S. scintillans* which belongs to the heterotrophic part (basal part) of the heterokont lineages is described following the International Zoological code (some information such as the type species have been added).

Symbiomonas **Guillou et Chrétiennot-Dinet, *genus novum***

Naked free-living heterotrophic uni-flagellated cells. No lorica. Flagellum with two rows of tubular flagellar hairs, each with two long terminal but no lateral filaments. No flagellar transitional helix. Endosymbiotic bacteria are enclosed inside an endoplasmic reticulum vesicle which is continuous with the outer membrane of the nuclear envelope. R3 root comparable to that of *Cafeteria roenbergensis* bicosoecid, except for the number of microtubules (6+3+x).

Type species: *Symbiomonas scintillans* Guillou et Chrétiennot-Dinet *sp. nov.*

Etymology: The name, *Symbiomonas,* refers to the endosymbiotic bacteria found inside the cell.

Symbiomonas scintillans **Guillou et Chrétiennot-Dinet, *species nova***

Characters of the genus. Spherical or ovoid cells, reduced in size, 1.4 µm in average diameter. Swimming is very slow. Collected by D. Vaulot during the OLIPAC cruise (Nov. 1994), in the equatorial Pacific Ocean at 150°00′W, 16°00′S and by F. Partensky during the MINOS cruise (June 1996), in the Mediterranean Sea at 11°21′E, 38°00′N.

Holotype: Fig. 1A

Etymology: Because swimming is very slow, cells seem to scintillate under an optical microscope.

Picophagus **Guillou et Chrétiennot-Dinet, new genus**

Characters of the genus. Tubular flagellar hairs with two terminal filaments. Flagella inserted at 90°. Nu-

cleus located above the basal body of the long flagellum.

Type species: *Picophagus flagellatus* Guillou et Chrétiennot-Dinet *sp. nov.*

Etymology: The name refers to the reduced size and the active predation by phagotrophy of the type species.

Sicut pro ordine. Mastigonemates tubulares cum binis filis terminalibus. Flagella bina, ad 90° inserta. Nucleus positus supra basalum corpum flagelli longioris.

Species typifica: Picophagus flagellatus Guillou et Chrétiennot-Dinet

***Picophagus flagellatus* Guillou et Chrétiennot-Dinet, new species**

Holotypus: Fig. 3A

Characters of the genus. Spherical or ovoid cells reduced in size, 1.8 µm in average diameter. The immature flagellum (F2) is very long, about 6 times longer than the cellular diameter. Active phagotroph. Collected by D. Vaulot during the OLIPAC cruise (Nov. 1994), in the equatorial Pacific Ocean at 150°00′W, 11°30′S.

Holotype: Fig. 3A

Etymology: The specific epithet refers to the long flagellum size compared to the cell diameter of this species.

Sicut genus. Cellulae sphaericae aut ovales, minutissimae, circiter 1,8 um in diametro. Flagellum (F2) corpus cellulae circa sex tanto longius. Nutricatione heterotrophica et efficiente. Per navigatione OLIPAC 1994, in Oceano Pacifico, (long. Occident. 150°00′, lat. austr. 11°30′), a D. Vaulot collectae.

Holotypus : Fig. 3A

Methods

Cultures: *S. scintillans* was isolated from the western Mediterranean Sea [11°20′E, 38°00′N, 5 m depth, 22 June 1996, strain RCC25 for Roscoff Culture Collection (RCC, Website 1999)] during the MINOS cruise and from the equatorial Pacific Ocean (150°00′W , 16°00′S, 20 m depth, 26 November 1994, strain RCC24) during the OLIPAC cruise. *P. flagellatus* was isolated from the equatorial Pacific Ocean (150°00′W, 11°50′S, 15 m depth, 7 November 1994, strain RCC22) during the OLIPAC cruise. Strains were further purified by serial dilution and maintained in K medium (Keller et al. 1987), at 19 °C, using 100 µmol quanta m^{-2} s^{-1}, under a 12:12 h light/dark regime. Light was provided by Sylvania Daylight fluorescent bulbs. All these strains are maintained without addition of organic matter, but can feed on free-living heterotrophic bacteria as the culture were non-axenic. These two strains also grow in darkness.

Transmission electron microscopy: For whole-mount preparations, cells were fixed for 15 min in a fixative solution containing 1–1.4% glutaraldehyde, 0.4 M cacodylate buffer (pH = 7.2), and 0.7% saccharose (final concentrations). A drop of fixed cells was deposited onto formvar-coated grids. After 10 min, most of the fluid was removed from the grids by capillarity. Cells were either stained with 1% uranyl acetate for 5 min and rinsed with distilled water, or allowed to dry for negative staining. For thin sections, 250 ml of cultures were fixed with the solution described above. Cells were harvested by centrifugation at 4,000 g, and the pellet was included into 1.5% purified agarose (Appligene, ref: 130021, Illkirch, France). Agarose blocks were then rinsed in 0.5 M cacodylate buffer and post-fixed with 1% OsO_4 and 0.5 M cacodylate buffer for 2 h. Cells were progressively dehydrated in ethanol and propylene oxide, then embedded into Spurr's resin. Photomicrographs were taken with a JEOL JEM-1200EX electron microscope.

Molecular analyses: Cells from two liters of culture were collected by centrifugation and resuspended into DNA extraction buffer (25% sucrose, 50 mM Tris, 1 mM EDTA). Cells were incubated 2 h with 0.4 mg ml^{-1} proteinase K at 37 °C. DNA was extracted using a standard phenol:chloroform protocol and alcohol precipitation. DNA was purified with the Geneclean II kit (BIO 101, La Jolla, California). The SSU rDNA of *Picophagus flagellatus* was sequenced first by Dr L. Medlin (Bremerhaven, Germany, for the protocol used see Guillou et al. 1999). This sequence was confirmed in the Roscoff laboratory, with the following protocol: the SSU rDNA was amplified by PCR with the following oligonucleotide primers: 5'-ACCTGGTTGATCCTGCCAG-3', 5'-TGATCCTTCYGCAGGTTCAC-3', complementary to regions of conserved sequences proximal to the 5' and 3' termini of the 18S rRNA gene (Moon-van der Staay et al. in press). The thermal cycle parameters were as follows: denaturation at 94 °C for 1 min (initial denaturation, 5 min), annealing at 55 °C for 2 min, extension at 72 °C for 3 min (final extension, 10 min). The reaction was cycled 30–35 times. PCR products were directly sequenced using the VISTRA automatic sequencer (Amersham, Les Ulis, France) and internal primers labelled with Texas Red (Amersham). In each case, the sequences were obtained without extra bands, suggesting that a single geno-

type was amplified. Both strands of each gene were sequenced.

These sequences were aligned with 56 others belonging to the Heterokonta for the first analyses (Fig. 6) and with 39 heterotrophic heterokonts for the second one (Fig. 7). *Alexandrium tamarense* (X54946), *Amphidinium belauense* (L13719), and *Prorocentrum minimum* (Y16238) sequences, belonging to the dinoflagellates, were used as outgroups. Alignments were built by visual inspection using the SEAVIEW software (Galtier et al. 1996) and with the help of the SSU rRNA secondary structure (for the model see Lange et al. 1996). These alignments are available on request. Highly variable gene regions were removed, leaving 1588 and 1554 of unambiguously aligned regions for the subsequent phylogenetic analyses respectively. Maximum likelihood analyses were conducted on both alignments using the fastDNAml software (version 1.0.6, Olsen et al. 1994). Distance analysis (neighbor-joining) and maximum parsimony methods were performed using the PHYLIP package (v. 3.57c Felsenstein 1985). The Kimura two-parameter option was employed to compute evolutionary distances (Kimura 1980). Bootstrap analyses (100 replicates, Felsenstein 1985) were conducted on both data sets with neighbor-joining and parsimony methods.

Acknowledgements

We thank S. Loiseaux-de Goër for help with the Heterokonta alignment, R.A. Andersen for the chrysophycean alignment, L. Medlin for independently confirming the *P. flagellatus* sequence, C.J. O'Kelly for help with microtubular flagellar roots, N. Simon for critically reading the manuscript, J. Sourimant for technical help with electron microscopy. Financial support for LG was provided by a doctoral fellowship from the Région Bretagne. This work was supported in part by the following programs: JGOFS-France (EPOPE and PROSOPE), Réseau Biodiversité Marine, GDR 869 (MINOS cruise), ACC-SV N°7, DFG (ME 1480/1-2) and PICODIV (EVK2-1999-00119).

References

Andersen RA, Wetherbee R (1992) Microtubules of the flagellar apparatus are active during prey capture in the chrysophycean alga *Epipyxis pulchra*. Protoplasma **166**: 8–20

Andersen RA, Brett RW, Potter D, Sexton JP (1998) Phylogeny of the Eustigmatophyceae based upon 18S rDNA, with emphasis on *Nannochloropsis*. Protist **149**: 61–74

Andersen RA, Saunders GW, Paskind MP, Sexton J (1993) Ultrastructure and 18S rRNA gene sequence for *Pelagomonas calceolata* gen. and sp. nov. and the description of a new algal class, the Pelagophyceae *classis nov.* J Phycol **29**: 701–715

Andersen RA, Barr DJS, Lynn DH, Melkonian M, Moestrup Ø, Sleigh MA (1991) Terminology and nomenclature of the cytoskeletal elements associated with the flagellar/ciliary apparatus in protists. Protoplasma **164**: 1–8

Andersen RA, VandePeer Y, Potter D, Sexton JP, Kawachi M, LaJeunesse T (1999) Phylogenetic analysis of the SSU rRNA from members of the Chrysophyceae. Protist **150**: 71–84

Barr DJS, Allan PME (1985) A comparison of the flagellar apparatus in *Phytophtora*, *Saprolegnia*, *Thraustochytrium*, and *Rhizidiomycetes*. Can J Bot **63**: 138–154

Barr DJS, Désaulniers NL (1989) The Flagellar Apparatus of the Oomycetes and Hyphochytriomycetes. In Green JC, Leadbeater BSC, Diver WL (eds). The Chromophyte Algae: Problems and Perspectives. Syst Assoc Spec Vol 38, Clarendon Press, Oxford, pp 343–355

Bhattacharya D, Medlin L (1995) The phylogeny of plastids: A review based on comparisons of small-subunit ribosomal RNA coding regions. J Phycol **31**: 489–498

Bourrelly P (1968) Les algues d'eau douce. II. Les algues jaunes et brunes. Boubée, Paris

Butcher RW (1952) Contribution to our knowledge of the smaller marine algae. J Mar Biol Assoc UK **31**: 175–191

Caron AC, Peele ER, Lin Lim E, Dennett MR (1999) Picoplankton and nanoplankton and their trophic coupling in surface waters of the Sargasso Sea south of Bermuda. Limnol Oceanogr **44**: 259–272

Daugbjerg N, Andersen RA (1997) A molecular phylogeny of the heterokont algae based on analyses of chloroplast-encoded *rbc*L sequence data. J Phycol **33**: 1031–1041

Delwiche CF, Kuhsel M, Palmer JD (1995) Phylogenetic analysis of *tuf*A sequences indicates a cyanobacterial origin of all plastids. Mol Phylog Evol **4**: 110–128

Dick MW (1990). Phylum Oomycota. In Margulis L, Corliss JO, Melkonian M, Chapman DJ (eds). Handbook of Protoctista. Jones and Bartlett Publ, Boston pp 661–685

Dick MW, Vick MC, Gibbings JG, Hedderson TA, Lastra CCL (1999) 18S rDNA for species of *Leptolegnia* and other Peronosporomycetes: justification for the subclass taxa Saprolegniomycetidae and Peronosporomycetidae and division of the Saprolegniaceae

sensu lato into the Leptolegniaceae and Saprolegniaceae. Mycol Res **103**: 1119–1125

Doddema H, van der Veer J (1983) *Ochromonas monicis* sp. nov. a particle feeder with bacterial endosymbionts. Cryptog Algol **4**: 89–97

Felsenstein J (1985) Confidence limits on phylogenies: an approach using the bootstrap. Evolution **39**: 783–791

Fenchel T, Patterson DJ (1988) *Cafeteria roenbergensis* nov. gen., nov. sp., a heterotrophic microflagellate from marine plankton. Mar Microb Food Webs **3**: 9–19

Galtier N, Gouy M, Gautier C (1996) SEAVIEW and PHYLO_WIN: two graphic tools for sequence alignment and molecular phylogeny. Comput Appl Biosci **12**: 543–548

Guillou L, Chrétiennot-Dinet MJ, Medlin LK, Claustre H, Loiseaux de Goër S, Vaulot D (1999) *Bolidomonas*: A new genus with two species belonging to a new algal class, the Bolidophyceae (Heterokonta). J Phycol **35**: 368–381

Hibberd DJ (1971) Observations on the cytology and ultrastructure of *Chrysamoeba radians* Klebs (Chrysophyceae). Br Phycol J. **6**: 207–223

Honda D, Yokochi T, Nakahara T, Raghukumar S, Nakagiri A, Schaumann K, Higashihara T (1999) Molecular phylogeny of labyrinthulids and thraustochytrids based on the sequencing of 18S ribosomal RNA gene. J Euk Microbiol **46**: 637–646

Johnson PW, Sieburth JM (1982) *In-situ* morphology and occurence of eucaryotic phototrophs of bacterial size in the picoplankton of estuarine and oceanic waters. J Phycol **18**: 318–327

Karpov SA, Kersanach R, Williams DM (1998) Ultrastructure and 18S rRNA gene sequence of a small heterotrophic flagellate *Siluania monomastiga* gen. et sp. nov. (Bicosoecida). Europ J Protistol **34**: 415–425

Keller MD, Selvin RC, Claus W, Guillard RRL (1987) Media for the culture of oceanic ultraphytoplankton. J Phycol **23**: 633–638

Kimura M (1980) A simple method for estimating evolutionary rates of base substitutions through comparative studies of nucleotide sequences. J Mol Evol **16**: 111–120

Lange M, Guillou L, Vaulot D, Simon N, Amann RI, Ludwig W, Medlin LK (1996) Identification of the class Prymnesiophyceae and the genus *Phaeocystis* with ribosomal RNA-targeted nucleic acid probes detected by flow cytometry. J Phycol **32**: 858–868

Leipe DD, Tong SM, Goggin CL, Slemenda SB, Pieniazek NJ, Sogin ML (1996) 16S-like rDNA sequences from *Developayella elegans*, *Labyrinthuloides haliotidis*, and *Proteromonas lacertae* confirm that the stramenopiles are a primarily heterotrophic group. Europ J Protistol **32**: 449–458

Li WKW, Subba Rao DV, Harrison WG, Smith JC, Cullen JJ, Irwin B, Platt T (1983) Autotrophic picoplankton in the tropical ocean. Science **219**: 292–295

Lim EL, Dennett MR, Caron DA (1999) The ecology of *Paraphysomonas imperforata* based on studies employing oligonucleotide probe identification in coastal water samples and enrichment cultures. Limnol Oceanogr **44**: 37–51

Moestrup Ø, Thomsen HA (1976) Fine structural studies on the flagellate genus *Bicoeca*. I. – *Bicoeca maris* with particular emphasis on the flagellar apparatus. Protistologica **12**: 101–120

Moon-van der Staay SY, van der Staay GWM, Guillou L, Claustre H, Medlin LK, Vaulot D (in press) Abundance and diversity of Prymnesiophyceae in the picoplankton community from the equatorial Pacific Ocean inferred from 18S rDNA sequences. Limnol Oceanogr

O'Kelly CJ, Patterson DJ (1996) The flagellar apparatus of *Cafeteria roenbergensis* Fenchel & Patterson, 1988 (Bicosoecales = Bicosoecida). Europ J Protistol **32**: 216–226

Olsen GJ, Matsuda H, Hagstrom R, Overbeek R (1994) fastDNAml: a tool for construction of phylogenetic trees of DNA sequences using maximum likelihood. Comput Appl Biosci **10**: 41–48

Patterson DJ (1985) The fine structure of *Opalina ranarum* (family Opalinidae): opalinid phylogeny and classification. Protistologica **21**: 413–428

Patterson DJ (1989). Stramenopiles: Chromophytes from a Protistan Perspective. In Green JC, Leadbeater BSC, Diver WL (eds). The Chromophyte Algae: Problems and Perspectives. Syst Assoc Spec Vol 38,Clarendon Press, Oxford, pp 357–379

Penna A, Magnani M (1999) Identification of *Alexandrium* (Dinophyceae) species using PCR and rDNA-targeted probes. J Phycol **35**: 615–621

Platt T, Subba Rao DV, Irwin B (1983) Photosynthesis of picoplankton in the oligotrophic ocean. Nature **300**: 702–704

Porter D (1990). Phylum Labyrinthulomycota. In Margulis L, Corliss JO, Melkonian M , Chapman DJ (eds). Handbook of Protoctista. Jones and Bartlett Publ, Boston, pp 388–398

Preisig HR, Hibberd DJ (1983) Ultrastructure and taxonomy of *Paraphysomonas* (Chrysophyceae) and related genera (3). Nord J Bot **3**: 695–723

Raven JA (1998) The twelfth Tansley Lecture. Small is beautiful: the picophytoplankton. Functional Ecology **12**: 503–513

Reckermann M, Veldhuis MJW (1997) Trophic interactions between picophytoplankton and micro- and nanozooplankton in the western Arabian Sea during the NE monsoon 1993. Aquat Microb Ecol **12**: 263–273

Ruinen J (1938) Notizen über Salzflagellaten. II. Über die Verbreitung der salzflagellaten. Arch Protistenkd **90**: 210–258

Saunders GW, Potter D, Andersen RA (1997) Phylogenetic affinities of the Sarcinochrysidales and Chrysomeridales (Heterokonta) based on analyses of molecular and combined data. J Phycol **33**: 310–318

Silberman JD, Sogin ML, Leipe DD, Clark CG (1996) Human parasite finds taxonomic home. Nature **380**: 398

Teal TH, Guillemette T, Chapman M, Margulis L (1998) *Acronema sippewissetensis* gen. nov. sp. nov., microbial mat bicosoecid (Bicosoecales = Bicosoecida). Europ J Protistol **34**: 402–414

Tong SM (1995) *Developayella elegans* nov. gen., nov. spec., a new type of heterotrophic flagellate from marine plankton. Europ J Protistol **31**: 24–31

Website Roscoff Culture Collection, RCC (January 1999, revision date) http://www.sb-roscoff.fr/Phyto/collect.html. 15 avril 1999, last date accessed